# Photocatalytic Degradation of Diazinon Using Titanium Oxide Synthesized by Alkaline Solvent

**Mohammad Rofik Usman[1,2], Atiek Rostika Noviyanti[1], and Diana Rakhmawaty Eddy[1,*]**

*[1]Department of Chemistry, Faculty of Mathematics and Natural Sciences, Universitas Padjadjaran, Jl. Raya Bandung-Sumedang km. 21, Jatinangor, Sumedang, West Java 45363 Indonesia*

*[2]Pharmacy Study Programme, Sekolah Tinggi Ilmu Kesehatan, Jl. Letkol Istiqlah No. 109 Banyuwangi, East Java 68422, Indonesia*

*Received August 3, 2016; Accepted December 22, 2016*

## ABSTRACT

*Photoactivity of titanium dioxide ($TiO_2$) can be improved by transformation to nanoparticles. Synthesis of $TiO_2$ nanoparticles can be accomplished by a hydrothermal method and the product of this method is affected by types of the precursor, reactant type, and concentration, also hydrothermal conditions, i.e. time and temperature. Titanium dioxide crystal nanoparticles can be applied to catalyze the degradation of insecticide, including diazinon. The objective of the present study was to determine the hydrothermal condition that produces high-quality $TiO_2$ crystals nanoparticles. In the present study, titanium tetrachloride ($TiCl_4$) was used as initial precursors while distilled water, double distilled water (DDW), ethanol, t-butanol, sodium hydroxide (NaOH) and potassium hydroxide (KOH) was used as reactants. The diffractogram of the $TiO_2$ nanoparticles showed anatase and rutile crystal structures. Based on calculations using the Scherrer equation, the $TiO_2$ crystals size were less than 50 nm for both anatase and rutile. The percentage of rutile and anatase composition was determined using Rietveld method assisted by rietica software. Morphology examination of $TiO_2$ crystals showed cubic and flower-shaped particles for anatase and rutile crystals, respectively. The best degradation performance of diazinon through photoactivity was given by $TiO_2$ synthesized using KOH as a reactant.*

***Keywords***: *titanium dioxide nanoparticles; hydrothermal; Scherrer equation; Rietveld method; diazinon*

## ABSTRAK

*Fotoaktivitas titanium dioksida ($TiO_2$) dapat ditingkatkan dengan mengubahnya menjadi nanopartikel. Sintesis nanopartikel $TiO_2$ dapat dilakukan dengan metode hidrotermal. Metode hidrotermal dipengaruhi oleh jenis prekursor, kondisi hidrotermal yang meliputi waktu, suhu, jenis dan konsentrasi reaktan. Kristal nanopartikel $TiO_2$ dapat digunakan untuk mengkatalisis degradasi insektisida, termasuk diazinon. Tujuan dari penelitian ini yaitu untuk memperoleh kondisi hidrotermal yang menghasilkan kristal $TiO_2$ nanopartikel dengan kualitas tinggi. Bahan yang digunakan yaitu titanium tetraklorida ($TiCl_4$) sebagai prekursor dan untuk jenis reaktan yang digunakan akuades, akuabides, etanol, t-butanol, natrium hidroksida (NaOH) dan kalium hidroksida (KOH). Difraktogram yang diperoleh menunjukkan kristal $TiO_2$ nanopartikel dengan struktur anatase dan rutile. Berdasarkan hasil perhitungan menggunakan persamaan Scherrer kristal $TiO_2$ nanopartikel yang diperoleh memiliki ukuran kristal di bawah 50 nm baik anatase maupun rutil. Persentase komposisi rutile dan anatase ditentukan dengan metode Rietveld menggunakan bantuan program rietica. Morfologi $TiO_2$ anatase menunjukkan partikel dalam bentuk kotak, sedangkan rutil berbentuk bunga. Kinerja degradasi diazinon melalui mekanisme fotoaktivitas ditunjukkan oleh $TiO_2$ yang disintesis menggunakan KOH.*

***Kata Kunci***: *titanium dioksida nanopartikel; hidrotermal; persamaan Scherrer; metode Rietveld; diazinon*

## INTRODUCTION

The heterogeneous photocatalyst is one of the effective and efficient solutions to solve environmental problems such as pollution caused by textile dyes [1-4] and pesticide waste [5-6]. One of widely used photocatalyst used is titanium dioxide ($TiO_2$). $TiO_2$ has a high band gap (approximately 3.23 eV) [7] and non-toxic [8]. The product of photodegradation organic molecules by $TiO_2$ finally is $CO_2$ and $H_2O$ [9]. Furthermore, $TiO_2$ can be used for pollution reduction on the air like $CO_2$, which produce other chemicals such as $CH_4$, $CH_3OH$, and $C_2H_2$ [10]. So $TiO_2$ can transform organic molecules hazardous to safety.

* Corresponding author. Tel : +62-8132-2731173
Email address : diana.rahmawati@unpad.ac.id

DOI: 10.22146/ijc.23548

There are three structure types of $TiO_2$ crystals, which are brookite, anatase, and rutile. Among the three structures, anatase showed the highest photoactivity, followed by rutile and brookite. Furthermore, the stability of anatase and rutile is higher than brookite, and therefore the anatase and rutile is often applied for practical purpose. The photoactivity of $TiO_2$ increases with increasing crystal surface area or with the decreasing particles size (nanoparticles) [11]. The synthesis pathway of $TiO_2$ nanoparticles can be performed using top-down or bottom-up pathways [12]. The bottom-up pathway can be performed by several methods such as hydrolysis [13], sol-gel [14-15] and hydrothermal [11,16]. In contrast to the top-down pathway, the bottom-up method requires sparse instrumentation.

Hydrothermal method is superior over to the other methods in term of high crystal quality and fast synthesis time [17]. A hydrothermal modification that has been done before that when mixing the precursor into the solvent. For example by sonication [18] and stirring [19] which required the shortest time each is 6 and 3 h. Therefore stirring simpler than sonication. At stirring begin can modify with increase temperature for shortening time like by increase temperature until 70 °C require time 1 h [20]. So as for this experiment will be used stirring and increase the temperature when stirring occurred before.

Titanium salt, such as titanium tetrachloride ($TiCl_4$), and titanium alkoxides of titanium tetra-isopropoxide (TTIP) are often used as $TiO_2$ nanoparticle precursor [21]. However, titanium salt precursor tends to form anatase $TiO_2$ nanoparticles exclusively [22]. Other factors than precursor type that can influence crystal quality, are hydrothermal conditions which include reactants type and concentration [16,23-24], reaction duration and hydrothermal temperature [18,23]. The Strong acid generated the best crystal size when acid was used as a reactant for the synthesis of $TiO_2$ nanoparticles [16]. However, when ethanol and the strong base was used, it was reported that the particle size of $TiO_2$ nanoparticles synthesized with strong base has a better size [25].

The purpose of the present study was to synthesize crystalline $TiO_2$ nanoparticles with the hydrothermal method using $TiCl_4$ as a precursor. The reactant type and concentration were varied to investigate its effect on crystals formed. The $TiO_2$ nanoparticle products were then used to degrade pesticide residue, i.e. diazinon. This pesticide was chosen because it has high toxicity and is still produced until today [26-27].

## EXPERIMENTAL SECTION

### Materials

The different solvents used in the present experiment were distilled water, double distilled water, ethanol (99%), *t*-butanol (99%), sodium hydroxide (NaOH), and potassium hydroxide (KOH). Titanium tetrachloride (99%) was used as a precursor. Ammonia ($NH_3$) (28%) was used to make an alkaline condition, while silver nitrate ($AgNO_3$) (99%) was used to detect the remaining chloride ion in the solution. *n*-Hexane (99%) was used to separate diazinon from the water. All reagents were purchased from Merck, except distilled water and double distilled water was purchased from the local chemical store and ammonia solution was purchased from APS Finechem. Titanium dioxide (99% crystal size 25 nm) as reference was purchased from Degussa and the crystal size of the synthesis products was compared to this reference.

### Instrumentation

Teflon Parr Instrument-47748 Autoclave was used for the hydrothermal process, Heidolph D91126 MR magnetic stirrer hotplate was used for stirring and heating solution, Mettler Toledo-MP220 digital pH meter was used for pH measurement, Beckman TJ-6 Centrifuge was used for particle separation, Carbolite S30 2RR Oven and Thermolyne-FB1310M furnace was used for water removal and impurity. Mettler Toledo AB164-S analytical balance was used to weigh samples. Crystal characterization was performed using XRD Philips Analytical-PW1710, PSA Vasco-114102, SEM JEOL JSM-6360LA. Data analysis were performed using rietica software (ver. 1.7.7) [28]. A reactor equipped with ultraviolet lamps was used as photodegradation chamber. Thermo Fisher Scientific Genesys 10S UV-vis spectrophotometer was used to determine diazinon concentration.

### Procedure

To 50 mL **A** (2 °C), 2 mL of 9 M $TiCl_4$ was added and stirred for a **B** h. After **C** min, the solution was heated to 50 °C. To achieve alkaline condition, 10 mL of 28% ammonia was added, followed by stirring. The suspension was then autoclaved for 24 h at 150 °C. The suspension was then centrifuged to separate the sediment after it was cooled. The sediment was collected and heated at 110 °C for 90 min followed by calcination for 2 h at **D** °C. The full condition of $TiO_2$ synthesis is presented in Table 1.

To 50 mL of 1000 ppm diazinon, 50 mg of $TiO_2$ (synthesis product and P25 Degussa as reference) was added and the suspension was irradiated using UV light with stirring for 1 h. The suspension was then decanted after the light was turned off. To 25 mL of decantation product, 20 mL of *n*-hexane was added to extract diazinon. This step was repeated three times. *n*-Hexane phase was pooled and dried until 5 mL remained. To the remaining *n*-hexane phase, *n*-hexane was added to give a final volume of 10 mL. The absorbance of diazinon was recorded using UV-vis spectrophotometer at a maximum wavelength of diazinon in *n*-hexane [29]. All $TiO_2$ product was tested for their photoactivity against diazinon degradation except T1 and T2.

### *Analysis*

The XRD patterns were analyzed by Scherrer equation (1) to obtain mean of crystal size [30].

$$d = \frac{K\lambda}{\beta \cos\theta} \quad (1)$$

where, d is mean of crystal size, β is FWHM, λ is the wavelength of X-radiation used and θ diffraction angle. The percentage composition of phase crystal structure obtained with Rietveld method using rietica software [31]. Standard of $TiO_2$ used data from Inorganic Crystal Structure Database (ICSD) with a number for anatase 172916 [32] and rutile 109469 [33].

The concentration of diazinon residue was converted to degradation percent (%) by equation (2).

$$D(\%) = \frac{C_0 - C_t}{C_0} \times 100\% \quad (2)$$

where, *D* is degradation percent while $C_0$ and $C_t$ is a concentration of diazinon before and after irradiation, respectively.

## RESULT AND DISCUSSION

XRD patterns of $TiO_2$ crystalline are shown in Fig. 1. Anatase phase of $TiO_2$ obtained has a crystal size

**Table 1.** Condition of $TiO_2$ synthesis hydrothermal method

| Condition | Reactant | Stirring Time (h) | Heating to 50 °C started after (min) | Calcinations temperature (°C) |
|---|---|---|---|---|
| | **A** | **B** | **C** | **D** |
| T1 | DDW | 3 | 60 | 350 |
| T2 | DDW | 3 | 60 | 600 |
| T3 | DDW | 1 | 30 | 600 |
| T4 | Distilled water | 1 | 30 | 600 |
| T5 | DDW: 96% ethanol (1:1) | 1 | 30 | 600 |
| T6 | DDW: ethanol (pa) (1:1) | 1 | 30 | 600 |
| T7 | DDW: *t*-butanol (pa) (1:1) | 1 | 30 | 600 |
| T8 | DDW: NaOH 0.5 M (1:1) | 1 | 30 | 600 |
| T9 | DDW: KOH 0.5 M (1:1) | 1 | 30 | 600 |

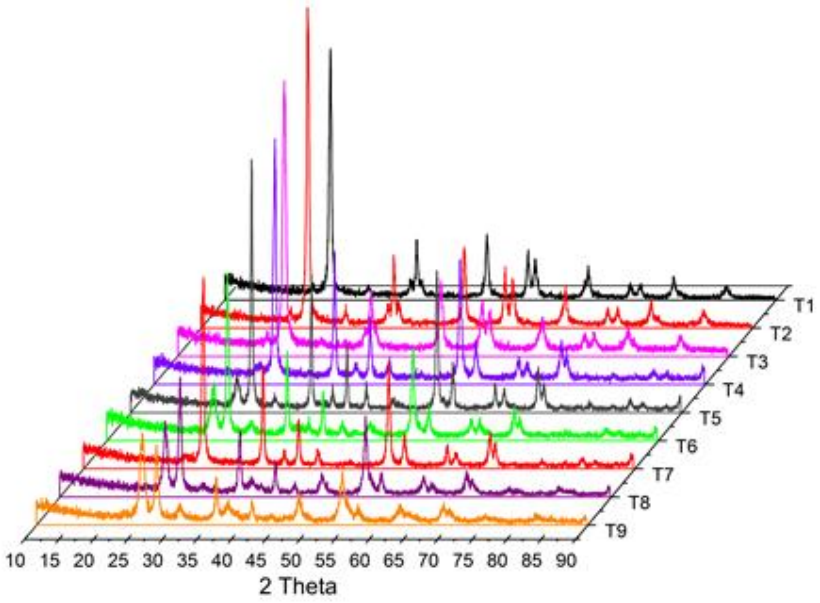


**Fig 1.** XRD patterns of $TiO_2$ results with $TiCl_4$ as initial precursor by hydrothermal method

**Table 2.** Phase and crystal size of $TiO_2$ synthesized with $TiCl_4$ as initial precursor by hydrothermal method

| Variant | Phase (%) | | Crystal Size (nm) | |
|---|---|---|---|---|
| | Anatase | Rutile | Anatase | Rutile |
| T1 | 100 | | 27.52 | |
| T2 | 100 | | 24.93 | |
| T3 | 100 | | 16.84 | |
| T4 | | 100 | | 37.87 |
| T5 | 81.28 | 18.72 | 20.98 | 44.96 |
| T6 | 81.28 | 18.72 | 19.07 | 38.99 |
| T7 | | 100 | | 41.51 |
| T8 | 81.34 | 18.66 | 22.34 | 36.31 |
| T9 | 81.33 | 18.67 | 14.92 | 26.99 |

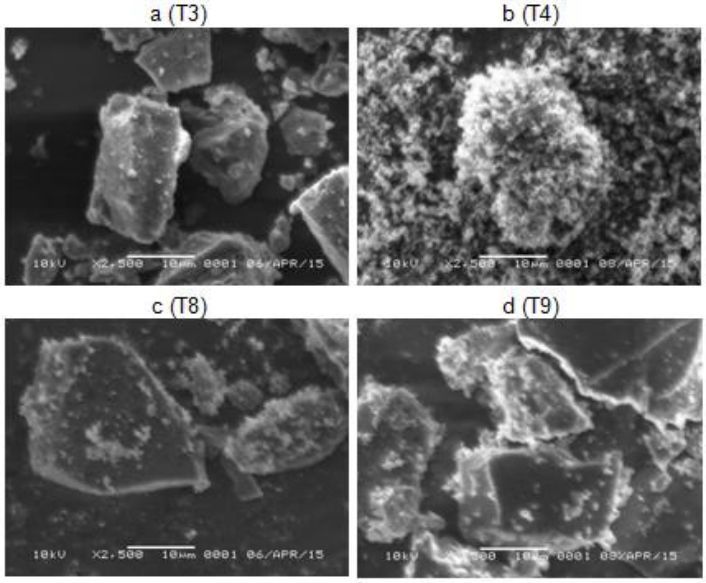


**Fig 2.** SEM image of $TiO_2$ synthesized with $TiCl_4$ as precursor by hydrothermal method (a: DDW (T3); b: aquadestilate (T4); c: DDW:NaOH 0.5 M (1:1) (T8); d: DDW:KOH 0.5 M (1:1) (T9)

smaller than rutile $TiO_2$ (see Table 2). We obtained a similar result to other studies [34-35] concerning the anatase to rutile phase transformation. The transformation of anatase to rutile phase gave an effect of surface interaction between two anatase particles. The interaction resulted in a rearrangement of anatase into rutile with larger crystal size. The crystal size of $TiO_2$ was compared to PSA with P25 Degussa. The smallest crystal size was observed for condition T9 (DDW:KOH 0.5 M (1:1)) (see Table 2). The particle size of formed $TiO_2$ crystal for condition T9 (520.30 nm) was smaller than P25 Degussa (1418.43 nm). The particle size increase showed $TiO_2$ agglomeration composed of large crystal size [36]. Thus crystal size T9 smaller than P25 Degussa. These events are shown on the morphology of $TiO_2$ (see Fig. 2a and b), where anatase (2a) are cubic shaped and rutile (2b) are flower-shaped. Thus, rutile would easily aggregate into particles with the larger size. Refined results of the two-phase $TiO_2$ anatase and rutile are shown in Table 3 and the refined results of XRD pattern are shown in Fig. 3.

**Calcination Temperature Effect**

Effect of calcination temperature can be resolved by comparing $TiO_2$ synthesis results between T1 and T2 in Table 2, where both conditions showed 100% anatase results. It occurred because at 600 °C, anatase $TiO_2$ produced by using reactants DDW was still stable [34,37]. The crystal size result showed a decrease ranging from 27.52-24.93 nm with the increase of calcination temperature of 350-600 °C. This was in accordance with the expected result because Cl atoms can not be eliminated completely at 350 °C [30], so it increases the volume of $TiO_2$ crystals.

**Stirring Duration Effect**

Duration of stirring showed an effect on crystal size. Longer stirring time increase crystal size, as shown by comparing the results of T2 and T3 in Table 2. Crystal size increased with the increasing stirring time, where dialysis occurred before the hydrothermal

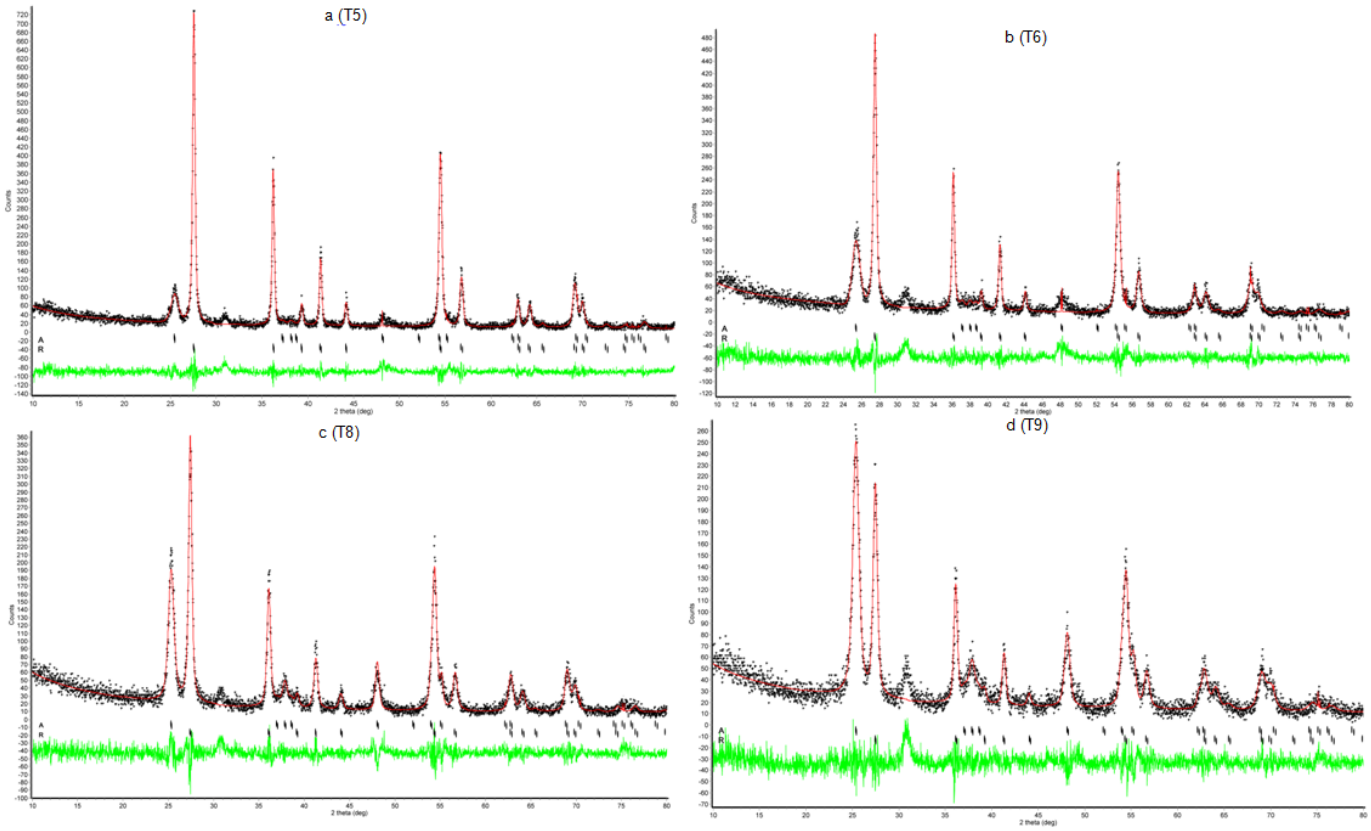


(Red Line: calculation data; green line: difference line; + point: experiment data; | point: marker point; A: anatase and R: rutile)

**Fig 3.** Rietveld refinement plot of $TiO_2$ using rietica (a: DDW:ethanol 96% (1:1) (T5); b: DDW:ethanol (pa) (1:1) (T6); c: DDW:NaOH 0.5M (1:1) (T8); d: DDW:KOH 0.5% (1:1) (T9))

**Table 3.** Refined parameters of $TiO_2$ nanoparticles by Rietveld method for T5: DDW:ethanol 96% (1:1); T6: DDW:ethanol (pa) (1:1); T8: DDW:NaOH 0.5M (1:1); T9: DDW:KOH 0.5% (1:1)

| Variant | Structure Parameter (nm) | | | Reliability Factor | | |
|---|---|---|---|---|---|---|
| | a | b | c | Rp | Rwp | $x^2$ |
| T5 (A) | 3.789 | 3.789 | 9.456 | 13.776 | 19.509 | 1.320 |
| T5 (R) | 4.598 | 4.598 | 2.957 | | | |
| T6 (A) | 3.783 | 3.783 | 9.473 | 14.564 | 19.933 | 1.521 |
| T6 (R) | 4.596 | 4.596 | 2.956 | | | |
| T8 (A) | 3.784 | 3.784 | 9.497 | 14.822 | 20.403 | 1.327 |
| T8 (R) | 4.592 | 4.592 | 2.958 | | | |
| T9 (A) | 3.784 | 3.784 | 9.509 | 14.475 | 20.392 | 1.404 |
| T9 (R) | 4.596 | 4.596 | 2.96 | | | |

A: anatase; R: rutile; Rp: profile residual factor; Rwp: weighted profile residual; $x^2$: goodness of fit (sometimes referred as chi-squared)

process. Aggregation was then occurred gradually forming a white precipitate. The aggregation size increase leads to increased crystal size of $TiO_2$ [13].

## Concentration Effect

Data T3, T4, T5 and T6 presented on Table 2 showed the effect of concentration on the crystal structure and size of $TiO_2$. $TiO_2$ crystals generated in water reactant as shown for T3 and T4 indicated that low concentrations used in the experiment causing unstable crystal structure so that T4 with the same calcination temperature transformed into rutile. In addition, the crystal size was also grown because of the phenomenon that has been described previously. Unlike T5 and T6 samples which used ethanol (96% and *p.a.* grade) as a reactant, $TiO_2$ crystal structure has a same weight percentage of anatase:rutile phase, which was 81.28%:18.72%. However, T6 crystal size is smaller than T5 for anatase and rutile phase. $TiO_2$

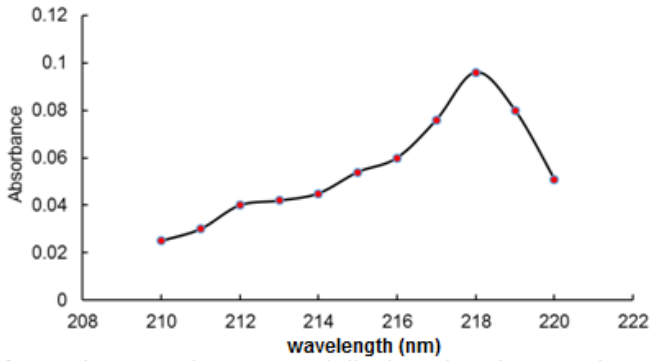


**Fig 4.** The scanning curve of diazinon in *n*-hexane (1000 ppm) by ultraviolet-visible spectrophotometer

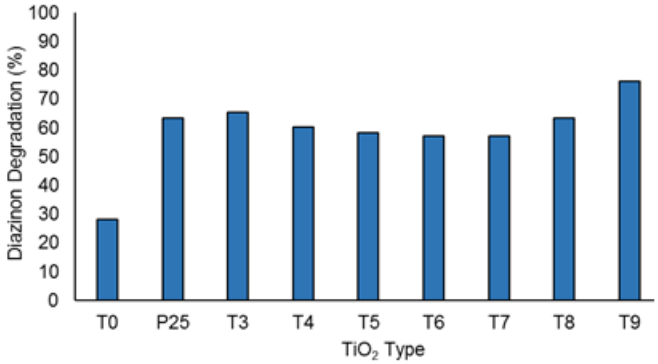


**Fig 5.** The activity of $TiO_2$ as photocatalyst in diazinon degradation (T0: without ultraviolet irradiation)

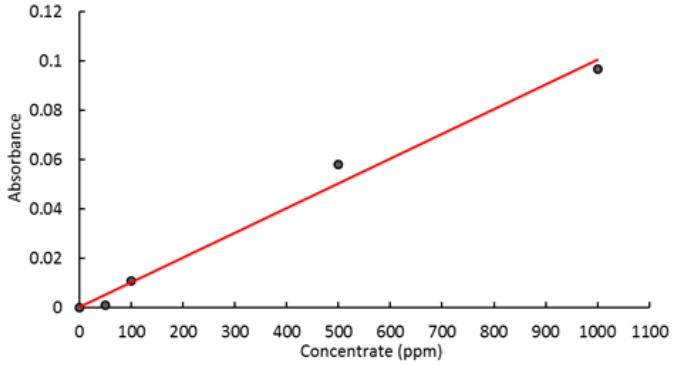


**Fig 6.** The standard curve of diazinon in *n*-hexane (0, 50, 100, 500, and 1000 ppm) by ultraviolet-visible spectrophotometer at 218 nm

produced by concentrated ethanol has smaller size because the amount of $OH^-$ also increased. Increasing $OH^-$ amount lead to increased interaction between two $Ti^{4+}$ ions that act as the central atom in $TiO_2$ [24]. In addition, the impact of $OH^-$ ions increases also causes the $TiO_2$ produced using $H_2O$ reactant has a smaller size in both anatase and rutile phase compared to ethanol. More $OH^-$ ions will be generated by $H_2O$ than ethanol.

### Reactant Type Effect

Data T3, T6, T7, T8 and T9 in Table 2 showed the influence of reactants type on the structure and crystal size of $TiO_2$. To explain the phenomenon of the reactant types, reactants were divided into several groups, which are reactants with a covalent bond ($H_2O$, ethanol, and *t*-butanol) and reactants with ionic bonds (NaOH and KOH). For reactant with a covalent bond, there is a trend where decreasing polarity will form $TiO_2$ with rutile structure and larger size (see data T7, T6 and T3 in Table 2, the polarity of *t*-butanol<ethanol<$H_2O$). Polarity properties of the reactants suggested that the types of reactant affected the $TiO_2$ crystals when $TiCl_4$ was used as a precursor in hydrothermal method [15].

In contrast to the reactants with covalent bonds, the reactants with ionic bond ionize in water perfectly and produce $OH^-$ ion. Since the capability of KOH in releasing $OH^-$ ion is higher than NaOH [38] thus, the crystal size of $TiO_2$ produced by using KOH is smaller for both anatase and rutile phases (see T8 and T9 in Table 2). In addition, the presence of KOH or NaOH will increase the growth of $TiO_2$ during the hydrothermal process [23]. The crystal structure is affected by cation size which showed the role of cation as impurity [39-40], where cation size increase lead to decrease the bond length of the crystal [40]. Thereby the formed crystals have a smaller size. T8 and T9 crystal structure have the same composition for both anatase and rutile (see Table 2). But the rutile structure T9 was more than T8, so the morphology of T9 (see Fig. 2d) has higher rutile particles than the morphology T8 (Fig. 2c).

### Photoactivity of $TiO_2$

The maximum wavelength of diazinon in *n*-hexane was scanned from 210 to 220 nm and maximum wavelength was observed at 218 nm (see Fig. 4). The linear equation form standard curve (see Fig. 5) is y=0.0001x+0.0003 with $r^2$=0.9878. Diazinon absorbance was calculated and converted to degradation percent (see Fig. 6). The highest degradation percentage was observed for T9 because it has the smallest particles size [11]. Degradation percentage is affected by particles size of $TiO_2$, where $TiO_2$ with small particles has more active site than $TiO_2$ with large particles [11]. T3 has degradation percentage higher than T8, although T8 is smaller. This might be due to its crystal state, where T8 has anatase structure. This result showed the percentage of anatase was influenced to diazinon degradation because anatase has band gap higher than rutile [41].

## CONCLUSION

Crystal of $TiO_2$ nanoparticles formed from $TiCl_4$ as an initial precursor with the hydrothermal method has an anatase, rutile, and anatase-rutile structure. The crystal size of $TiO_2$ calculated using Scherrer equation showed the product size less than 50 nm for all variation. The most stable $TiO_2$ anatase at 600 °C, was generated using DDW. While $TiO_2$ with the smallest crystal size either for anatase or rutile structure was formed when KOH was used. Increasing reactants polarity will lead to anatase structure formation. In addition, the $OH^-$ concentration of the reactants generated was also higher when KOH used, so $TiO_2$ formed anatase structure. Big cation and higher calcination temperature will lead to smaller crystal size. While longer stirring time before the hydrothermal process will produce a larger crystal size. Smaller particles of $TiO_2$ and more anatase will lead to a higher percent of diazinon degradation.

## ACKNOWLEDGEMENT

The present work was supported by Direktorat Jenderal Pendidikan Tinggi (DIKTI) through Beasiswa Program Pascasarjana Dalam Negeri (BPP-DN) to Mohammad Rofik Usman (Phone. (021)57946053, Fax (021)57946052, e-mail: bpp-dn@dikti.go.id).

## REFERENCES

[1] Carneiro, P.A., Osugi, M.E., Sene, J.J., Anderson, M.A., and Zanoni, M.V.B., 2004, Evaluation of color removal and degradation of a reactive textile azo dye on nanoporous $TiO_2$ thin-film electrodes, *Electrochim. Acta*, 49 (22-23), 3807–3820.

[2] Prieto, O., Fermoso, J., Nuñez, Y., del Valle, J.L., and Irusta, R., 2005, Decolouration of textile dyes in wastewaters by photocatalysis with $TiO_2$, *Sol. Energy*, 79 (4), 376–383.

[3] Pekakis, P.A., Xekoukoulotakis, N.P., and Mantzavinos, D., 2006, Treatment of textile dyehouse wastewater by $TiO_2$ photocatalysis, *Water Res.*, 40 (6), 1276–1286.

[4] Manurung, P., Situmeang, R., Ginting, E., and Pardede, I., 2015, Synthesis and characterization of titania-rice husk silica composites as photocatalyst, *Indones. J. Chem.*, 15 (1), 36–42.

[5] Lhomme, L., Brosillon, S., and Wolbert, D., 2008, Photocatalytic degradation of pesticides in pure water and a commercial agricultural solution on TiO2 coated media, *Chemosphere*, 70 (3), 381–386.

[6] Affam, A.C., and Chaudhuri, M., 2013, Degradation of pesticides chlorpyrifos, cypermethrin and chlorothalonil in aqueous solution by $TiO_2$ photocatalysis, *J. Environ. Manage.*, 130, 160–165.

[7] Valencia, S., Marín, J.M., and Restrepo, G., 2010, Study of the bandgap of synthesized titanium dioxide nanoparticules using the sol-gel method and a hydrothermal treatment, *TOMSJ*, 4, 9–14.

[8] Massard, C., Boudeaux, D., Raspal, V., Feschet-Chassot, E., Sibaud, Y., Caudron, E., Devers, T., and Awitor, K.O., 2012, O*ne-pot* synthesis of $TiO_2$ nanoparticles in suspensions for quantification of titanium debris release in biological liquids, *ANP*, 1, 86–94.

[9] Maryani, Y., and Kustiningsih, I., 2015, Determination and characterization of photocatalytic products of linear alkyl sulphonate by high performance liquid chromatography and nuclear magnetic resonance, *Procedia Chem.*, 17, 216–223.

[10] Zuas, O., Kim, J.S., and Gunlazuardi, J., 2014, Influence of operational parameters on the photocatalytic activity of powdered $TiO_2$ for the reduction of $CO_2$, *Indones. J. Chem.*, 14 (2), 122–130.

[11] Castro, A.L., Nunes, M.R., Carvalho, A.P., Costa, F.M., and Florêncio, M.H., 2008, Synthesis of anatase $TiO_2$ nanoparticles with high temperature stability and photocatalytic activity, *Solid State Sci.*, 10 (5), 602–606.

[12] Madhumitha, G., and Roopan, S.M., 2013, Devastated crops: Multifunctional efficacy for the production of nanoparticles, *J. Nanomater.*, 2013, 1–12.

[13] Abbas, Z., Holmberg, J.P., Hellström, A.K., Hagström, M., Bergenholtz, J., Hassellöv, M., and Ahlberg, E., 2011, Synthesis, characterization and particle size distribution of $TiO_2$ colloidal nanoparticles, *Colloids Surf., A*, 384 (1-3), 254–261.

[14] Zhang, Y., Xiong, G., Yao, N., Yang, W., and Fu, X., 2001, Preparation of titania-based catalysts for formaldehyde photocatalytic oxidation from $TiCl_4$ by the sol–gel method, *Catal. Today*, 68 (1-3), 89–95.

[15] Behnajady, M.A., Eskandarloo, H., Modirshahla, N., and Shokri, M., 2011, Investigation of the effect of sol–gel synthesis variables on structural and photocatalytic properties of $TiO_2$ nanoparticles, *Desalination*, 278 (1-3), 10–17.

[16] Kolen'ko, Y.V., Churagulov, B.R., Kunst, M., Mazerolles, L., and Colbeau-Justin, C., 2004, Photocatalytic properties of titania powders prepared by hydrothermal method, *Appl. Catal., B*, 54 (1), 51–58.

[17] Hanaor, D.A.H., and Sorrell, C.C., 2010, Review of the anatase to rutile phase transformation, *J. Mater. Sci.*, 46 (4), 855–874.
[18] Collazzo, G.C., Jahn, S.L., Carreño, N.L.V., and Foletto, E.L., 2011, Temperature and reaction time effects on the structural properties of titanium dioxide nanopowders obtained via the hydrothermal method, *Braz. J. Chem. Eng.*, 28 (2), 265–272.
[19] Zhang, J., Xiao, X., and Nan, J., 2010, Hydrothermal-hydrolysis synthesis and photocatalytic properties of nano-$TiO_2$ with an adjustable crystalline structure, *J. Hazard. Mater.*, 176 (1-3), 617–622.
[20] Lee, H.Y., and Kale, G.M., 2008, Hydrothermal synthesis and characterization of nano-$TiO_2$, *Int. J. Appl. Ceram. Technol.*, 5 (6), 657–665.
[21] Parra, R., Góes, M.S., Castro, M.S., Longo, E., Bueno, P.R., and Varela, J.A., 2008, Reaction pathway to the synthesis of anatase via the chemical modification of titanium isopropoxide with acetic acid, *Chem. Mater.*, 20 (1), 143–150.
[22] Seok, S.I., Vithal, M., and Chang, J.A., 2010, Colloidal $TiO_2$ nanocrystals prepared from peroxotitanium complex solutions: Phase evolution from different precursors, *J. Colloid Interface Sci.*, 346 (1), 66–71.
[23] Yin, H., Wada, Y., Kitamura, T., Sumida, T., Hasegawa, Y., and Yanagida, S., 2002, Novel synthesis of phase-pure nano-particulate anatase and rutile $TiO_2$ using $TiCl_4$ aqueous solutions, *J. Mater. Chem.*, 12 (2), 378–383.
[24] Oh, J.K., Lee, J.K., Kim, S.J., and Park, K.W., 2009, Synthesis of phase and shape-controlled $TiO_2$ nanoparticles via hydrothermal process, *J. Ind. Eng. Chem.*, 15 (2), 270–274.
[25] Wang, Y., Zhang, L., Deng, K., Chen, X., and Zou, Z., 2007, Low temperature synthesis and photocatalytic activity of rutile $TiO_2$ nanorod superstructures, *J. Phys. Chem. C*, 111 (6), 2709–2714.
[26] WHO, 2010, *The WHO Recommended Classification of Pesticides by Hazard and Guidelines to Classification 2009*, International Programme on Chemical Safety, Stuttgart.
[27] Ditjen PSP, 2012, *Pestisida Terdaftar dan Diizinkan*, Bagian Evaluasi dan Pelaporan, Jakarta.
[28] Hunter, B.A., 1997, *Rietica for Windows*, ver.1.7.7.
[29] Rahayu, W.S., Hartanti, D., and Handoyo, 2016, Analisis residu pestisida organofosfat pada simplisia temulawak (*Curcuma xanthorrhiza* Roxb.) dengan metode spektrofotometri visibel, *Pharmacy*, 6 (3), 1–10.
[30] Hayle, S.T., and Gonfa, G.G., 2014, Synthesis and characterization of titanium oxide nanomaterials using sol-gel method, *Am. J. Nanosci. Nanotechnol.*, 2 (1), 1–7.
[31] Wang, X.Y., Liu, Z., Liao, H., Klein, D., and Coddet, C., 2005, Deoxidisation and phase analysis of plasma sprayed $TiO_2$ by X-ray Rietveld method, *Thin Solid Films*, 473 (2), 177–184.
[32] Inorganic Crystal Structure Database (ICSD), 172916, 2008, United States.
[33] Inorganic Crystal Structure Database (ICSD), 109469, 2007, United States.
[34] Bakardjieva, S., Šubrt, J., Štengl, V., Dianez, M.J., and Sayagues, M.J., 2005, Photoactivity of anatase–rutile $TiO_2$ nanocrystalline mixtures obtained by heat treatment of homogeneously precipitated anatase, *Appl. Catal., B*, 58 (3-4), 193–202.
[35] Zhang, H., and Banfield, J.F., 1999, New kinetic model for the nanocrystalline anatase-to-rutile transformation revealing rate dependence on number of particles, *Am. Mineral.*, 84, 528–535.
[36] Suttiponparnit, K., Jiang, J., Sahu, M., Suvachittanont, S., Charinpanitkul, T., and Biswas, P., 2011, Role of surface area, primary particle size, and crystal phase on titanium dioxide nanoparticle dispersion properties, *Nanoscale Res. Lett.*, 6 (27), 1–8.
[37] Ou, H.H., and Lo, S.L., 2007, Review of titania nanotubes synthesized via the hydrothermal treatment: Fabrication, modification, and application, *Sep. Purif. Technol.*, 58 (1), 179–191.
[38] Sikhwivhilu, L.M., Ray, S.S., and Coville, N.J., 2008, Influence of bases on hydrothermal synthesis of titanate nanostructures, *Appl. Phys. A*, 94 (4), 963–973.
[39] Mao, X., Song, X., Lu, G., Sun, Y., Xu, Y., and Yu, J., 2014, Effects of metal ions on crystal morphology and size of calcium sulfate whiskers in aqueous HCl solutions, *Ind. Eng. Chem. Res.*, 53 (45), 17625–17635.
[40] Song, S.Y., and Ok, K.M., 2015, Modulation of framework and centricity: cation size effect in new quaternary selenites, $ASc(SeO_3)_2$ (A = NA, K, Rb, and Cs), *Inorg. Chem.*, 54 (10), 5032–5038.
[41] Landmann, M., Rauls, E., and Schmidt, W.G., 2012, The electronic structure and optical response of rutile, anatase and brookite $TiO_2$, *J. Phys. Condens. Matter.*, 24 (19), 1–6.